Secondary structure of the yeast Saccharomyces cerevisiae pre-U3A snoRNA and its implication for splicing efficiency

A. Mougin, A. Gregoire, J. Banroques, V. Segault, R. Fournier, F. Brule, M. Chevrier-Miller and C. Branlant

RNA 1996 2: 1079-1093

RNA (1996), 2:1079–1093. Cambridge University Press. Printed in the USA.

Secondary structure of the yeast *Saccharomyces cerevisiae* pre-U3A snoRNA and its implication for splicing efficiency

ANNIE MOUGIN,[1] ANNE GRÉGOIRE,[1] JOSETTE BANROQUES,[2] VÉRONIQUE SÉGAULT,[1] RÉGIS FOURNIER,[1] FABIENNE BRULÉ,[1] MARIANNE CHEVRIER-MILLER,[3] and CHRISTIANE BRANLANT[1]

[1] Laboratoire d'Enzymologie et de Génie Génétique, URA CNRS 457, Université de Nancy I, Faculté des Sciences, Boulevard des Aiguillettes, BP 239, 54506 Vandoeuvre-lès-Nancy cedex, France
[2] Centre de Génétique Moléculaire, CNRS, Avenue de la Terrasse, 91198 Gif sur Yvette, France
[3] Laboratoire de Génétique Moléculaire, Ecole Normale Supérieure, 46, rue d'Ulm, 75230 Paris cedex 05, France

ABSTRACT

The *Saccharomyces cerevisiae* U3 snoRNA genes contain long spliceosomal introns with noncanonical branch site sequences. By using chemical and enzymatic methods to probe the RNA secondary structure and site-directed mutagenesis, we established the complete secondary structure of the U3A snoRNA precursor. This is the first determination of the complete secondary structure of an RNA spliced in a spliceosome. The peculiar cruciform structure of the U3A snoRNA 3′-terminal region is formed in the precursor RNA and the conserved Boxes B and C are accessible for binding the U3 snoRNP proteins. The intron forms a highly folded structure with a long central stem-loop structure that brings the 5′ box and the branch site together. This is in agreement with the idea that secondary structure interactions are necessary for efficient splicing of long introns in yeast. The 3′ splice site is in a bulged loop and the branch site sequence is single-stranded. Surprisingly, the 5′ splice site is involved in a 6-base pair interaction. We used in vitro splicing experiments to show that, despite a noncanonical branch site sequence and a base paired 5′ splice site, transcripts that mimic the authentic pre-U3A snoRNA are spliced very efficiently in vitro. Sequestering the 5′ splice site in a more stable structure had a negative effect on splicing, which was partially compensated by converting the branch site sequence into a canonical sequence. Analysis of spliceosomal complex formation revealed a cumulative negative effect of a base pair interaction at the 5′ splice site and of a deviation to the consensus sequence at the branch site on the efficiency of spliceosome formation in vitro.

Keywords: RNA secondary structure; *S. cerevisiae*; splicing; U3 snoRNA

INTRODUCTION

In vertebrates, most of the nuclear genes coding for proteins contain several introns that can be up to 100 kb in length (Hawkins, 1988). The situation is very different in yeast. Introns spliced in a spliceosome are present in less than 5% of the *Saccharomyces cerevisiae* nuclear genes (Kalogeropoulos, 1995). Except for the MATα1 and the YL8A genes (Miller, 1984; Mizuta et al., 1992), the *S. cerevisiae* nuclear genes contain no more than a single intron. In addition to protein genes, a few yeast nuclear genes that code for metabolically stable RNAs contain introns that are spliced in a spliceosome. Such introns were first observed in the spliceosomal U6 snRNA gene from *Schizosaccharomyces pombe* (Tani & Ohshima, 1989) and the nucleolar U3 snoRNA genes from *S. cerevisiae* (Myslinski et al., 1990). Later, these introns were found in the U6 snRNA genes of other *Schizosaccharomyces* species, *Rhodotorula hasegawae* and *Rhodosporidium dacryoidum* (Tani & Ohshima, 1991), and in the U2 snRNA genes from *R. hasegawae* (Takahashi et al., 1993). A growing number of small nucleolar RNAs (snoRNAs) is characterized in *S. cerevisiae* (for review, see Maxwell & Fournier, 1995). However, only the U3A and U3B snoRNA genes were

Reprint requests to: Christiane Branlant, Laboratoire d'Enzymologie et de Génie Génétique, URA CNRS 457, Faculté des Sciences, Université de Nancy I, Boulevard des Aiguillettes, BP 239, 54506 Vandoeuvre-lès-Nancy cedex, France; e-mail: cbranlant@legg.u-nancy.fr.

found to contain an intron, and the introns of these two genes share the peculiarity of having a noncanonical sequence at the branch site (GACTAACp instead of TACTAACp) (Myslinski et al., 1990).

U3 snoRNA plays a crucial role in pre-ribosomal RNA maturation. In eukaryotes, the 18S, 5.8S, and 25/28S ribosomal RNAs (rRNAs) are transcribed by RNA polymerase I as a single precursor molecule. A complex series of processing reactions is needed to eliminate the 5′ and 3′ external transcribed spacers (5′ ETS and 3′ ETS, respectively) and the internal transcribed spacers 1 and 2 (Eichler & Craig, 1994; Maxwell & Fournier, 1995; Raué & Planta, 1995). The primary event, A_0 cleavage within the 5′ ETS spacer (Craig et al., 1987; Kass et al., 1987; Hughes & Ares, 1991), was reproduced successfully in extracts of cultured mouse cells (Craig et al., 1987) and in *Xenopus laevis* (Mougey et al., 1993), and it was found to be impaired upon U3 snoRNA depletion (Kass et al., 1990; Mougey et al., 1993). In yeast, when U3 snoRNAs are depleted, the normal pre-rRNA intermediates in the pathway leading to the synthesis of the 18S rRNA are missing, which results in an under-accumulation of mature 18S rRNA (Hughes & Ares, 1991).

Previously, we studied the secondary structure of the mature U3A snoRNA from *S. cerevisiae* (Ségault et al., 1992). It was interesting to compare this structure with that of the precursor RNA containing the intron. Up to now, only the secondary structures of limited portions of eukaryotic pre-mRNAs have been studied (Teare & Wollenzien, 1989, 1990; Clouet d'Orval et al., 1991; Li et al., 1995). However, several reports suggest an important role of RNA secondary structure in the splicing efficiency of yeast pre-mRNAs. Computer analysis suggested the presence of a long central stem-loop structure in several *S. cerevisiae* pre-mRNA introns (cyh2, S10, RP51A, and actin; Parker & Patterson, 1987). Moreover, the genetic deletion experiments of Pikielny and Rosbash (1985) and Newman (1987) suggested that a base pair interaction between segments located downstream from the 5′ splice site element and upstream of the branch point sequence is required for optimal splicing efficiency. This was confirmed experimentally by mutational analyses of the introns in the cyh2 ribosomal protein gene (Newman, 1987), and in the RP51B ribosomal protein gene (Goguel & Rosbash, 1993). Libri et al. (1995) recently proposed that base pair interactions are needed generally for efficient splicing of long introns in yeast, based on randomization selection experiments. Finally, two other examples showing the importance of pre-mRNA secondary structure on splicing efficiency in yeast are the occlusion of a 3′ splice site by the formation of a stable secondary structure in the *Kluyveromyces lactis* actin gene (Deshler & Rossi, 1991), and the auto-control of the *S. cerevisiae* L32 gene by the L32 protein binding on a stem-loop structure formed by the intron and the first exon (Eng & Warner, 1991). However, all these studies suffer from the absence of information about the entire secondary structure of the intron.

In this paper, we describe the complete secondary structure of the *S. cerevisiae* pre-U3A snoRNA. This precursor RNA is highly folded; it has a long central stem-loop structure in the intron and an unexpected 5′ stem-loop structure that contains the 5′ splice site. We also tested the importance of this unexpected 5′ stem-loop structure and the importance of the noncanonical branch site sequence on splicing efficiency. For this purpose, we produced variant pre-U3A snoRNAs by site-directed mutagenesis, and we studied their secondary structure and in vitro splicing efficiency. The possible implications of these two peculiar features of the pre-U3A snoRNA are discussed.

RESULTS

Strategy for secondary structure analysis

The intron of the *S. cerevisiae* U3A snoRNA gene is located in the region coding for the 5′-terminal stem-loop structure 1a (Myslinski et al., 1990; Ségault et al., 1992) (inset in Fig. 1A), which is supposed to play an essential role in pre-ribosomal RNA maturation (Beltrame & Tollervey, 1992, 1995). Exon 2 contains the sequence that forms the stem-loop structure 1b and the 3′-terminal cruciform structure in the mature RNA (inset in Fig. 1A). All the sequences expected to be required for binding of the U3 snoRNP proteins are contained in exon 2 (Parker & Steitz, 1987; Lübben et al., 1993; Hartshorne & Agabian, 1994; our unpubl. results on the yeast U3 snoRNP).

To determine the secondary structure of the pre-U3A snoRNA, we produced an in vitro transcript that contained a minimal number of extraneous nucleotides compared to the authentic pre-U3A snoRNA: two additional G residues at the 5′ end, to enhance transcription by T7 RNA polymerase, and one additional U residue at the 3′ end, which was generated by *Hpa* I digestion of the DNA template. This transcript contained a GACUAACp sequence at the branch site and a 16-nt long exon 1, and it was designated pU3G16.

The secondary structure was probed with dimethylsulfate (DMS), 1-cyclohexyl-3-(2-morpholino ethyl)-carbodiimide-metho-*p*-toluene sulfonate (CMCT), and S1 and V1 RNases, under the conditions given in the Materials and methods. Positions of modification or cleavage were identified by reverse transcription using primers 1, 2, and 3 (Figs. 1A, 2A). As will be described below, based on the properties of these agents (Ségault et al., 1992), two possible secondary structures of the pre-U3A snoRNA were deduced. Therefore, we constructed pre-U3A snoRNA variants by site-directed mutagenesis to test these two possibilities. These variant U3A pre-snoRNA transcripts were subjected to

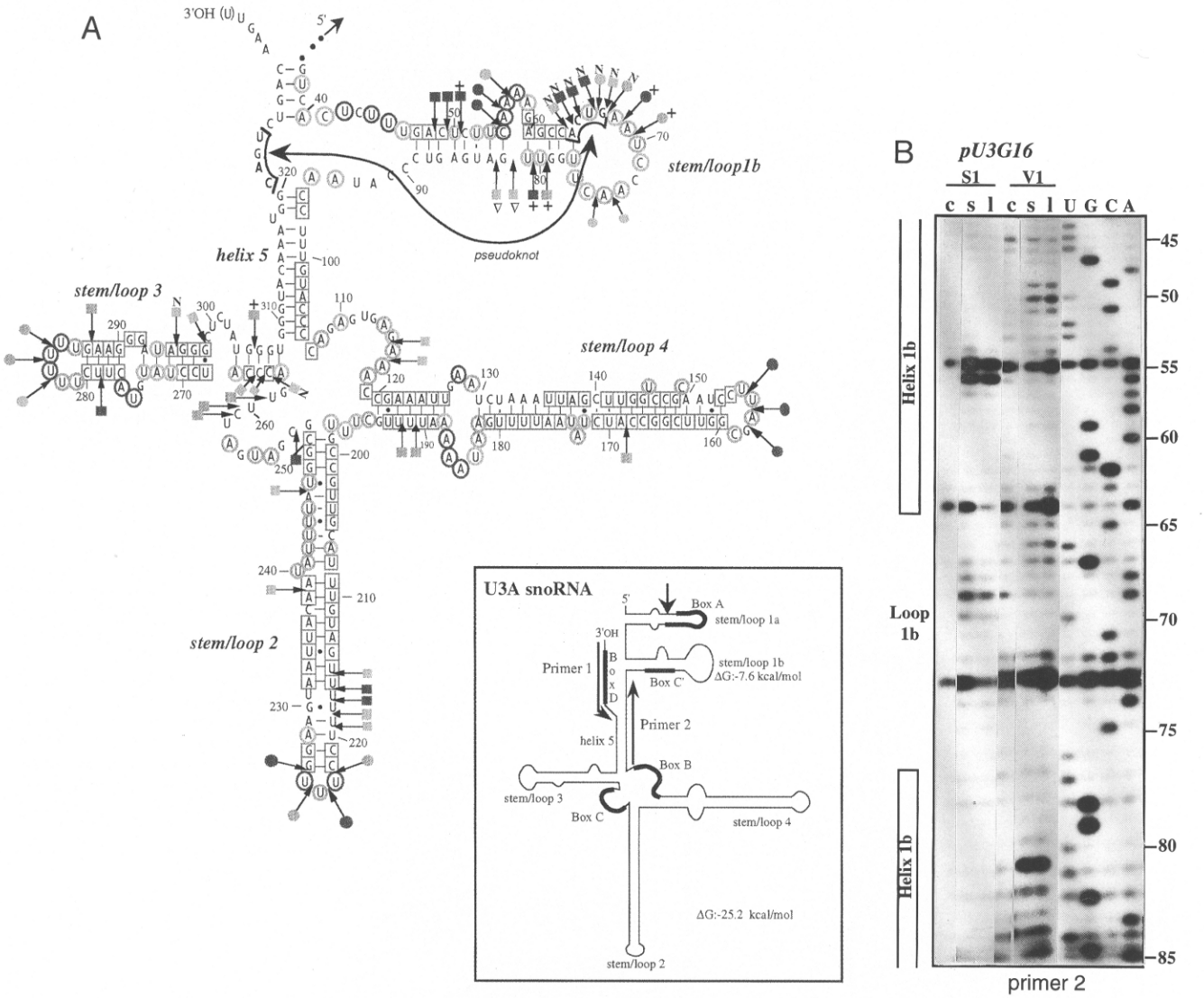

FIGURE 1. Secondary structure analysis of exon 2. Transcript pU3G16 was subjected to chemical (DMS and CMCT) and enzymatic (V1 and S1 nucleases) probing of the RNA secondary structure, under nondenaturing conditions. Positions of chemical modifications and enzymatic cleavages were identified by primer extension analysis with primers 1 and 2 (inset in **A**). The stem-loop structure nomenclature is according to Ségault et al. (1992). The location of the five phylogenetically conserved boxes, A, B, C, C′, and D (for review, see Maxwell & Fournier, 1995), and the calculated free energies of the stem-loop 1b and of the cruciform structure are shown in the inset of A. The results of probing experiments are represented schematically on the proposed exon 2 structure in A. Nucleotides modified by DMS or CMCT are circled. Colors of the circles indicate the intensity of modification: green, orange, and red for low, medium, and strong, respectively. Nucleotides in blue squares were never modified by chemical reagents. Arrows linked to a circle and arrows linked to a square indicate S1 RNase and V1 RNase cleavages, respectively. Colors of squares and circles indicate the yield of cleavage with the same rules as for chemical modifications. Differences of enzymatic cleavages in the precursor RNA as compared to the mature RNA are represented as follows: Δ, decreased cleavage intensity; +, increased cleavage intensity; N, a new cleavage. **B:** Accessibility to S1 and V1 nucleases of pU3G16 transcript from position 45 to 85 is analyzed by primer extension with primer 2. Lane c, control lane without enzyme; lane s, short incubation time (2 or 7 min for V1 and 12 min for S1); lane l, long incubation time (10 min for V1 and 25 min for S1). Lanes A, C, G, and U show the sequencing ladder of the respective nucleotide. Positions of loop and helix are indicated on the left of the panel.

RNA secondary structure analysis and the results allowed us to propose a complete secondary structure model for the pre-U3A snoRNA. For reasons of clarity, the positions of residues within exon sequences will be numbered as in the mature U3A snoRNA (Ségault et al., 1992), and those within the intron in italic numbers from *+1* to *+157*.

U3 snoRNA 3′-terminal cruciform structure and stem-loop structure 1b are found in the precursor RNA

For a comparative analysis between precursor and mature RNAs, the pU3G16 transcript and an in vitro U3 transcript produced as described previously (Ségault

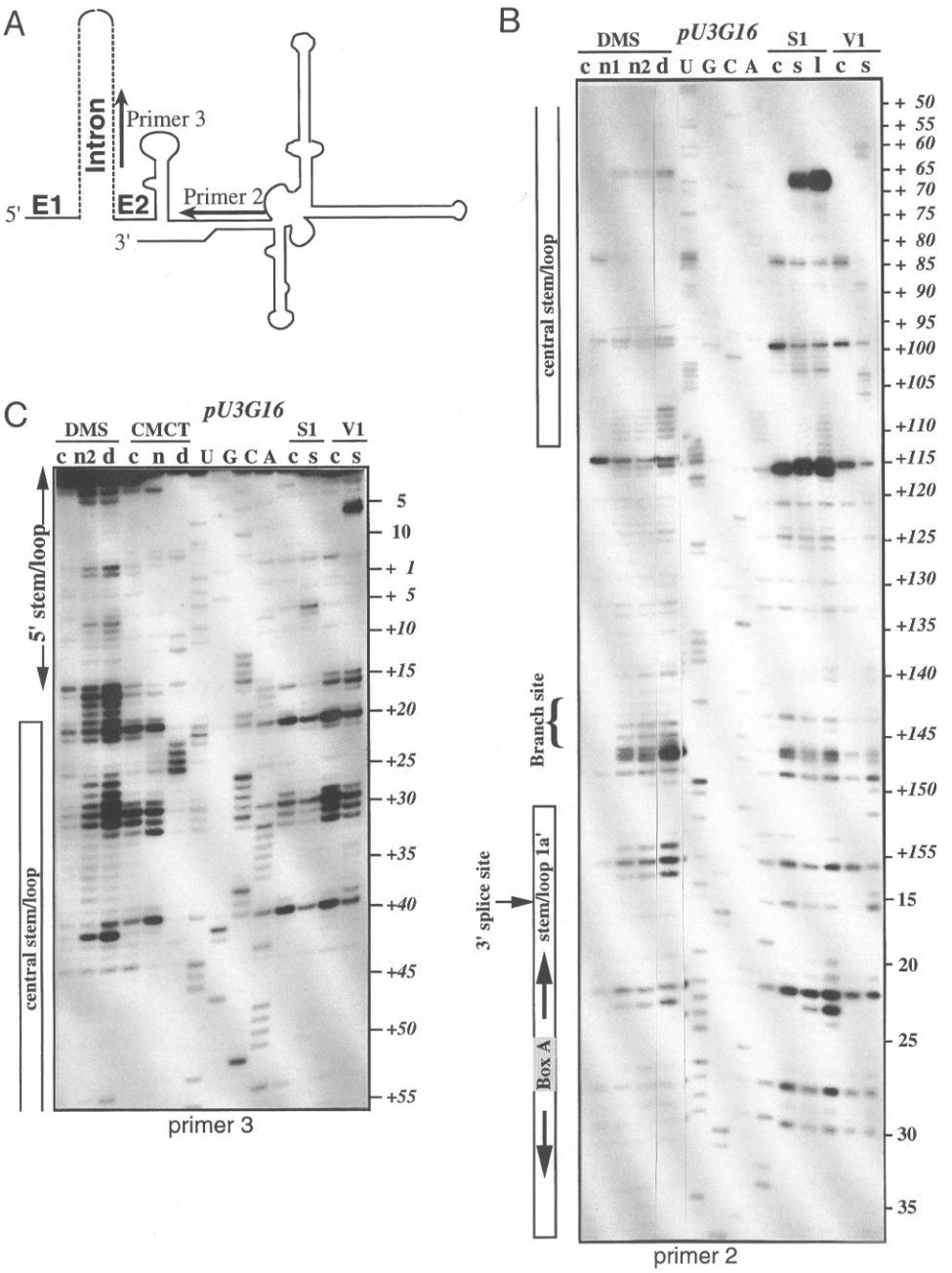

FIGURE 2. Chemical and enzymatic probing of the intron and exon 1 secondary structure. The pU3G16 transcript was digested with S1 and V1 nucleases (same nomenclature of the lanes as in Fig. 1) and modified with DMS or CMCT chemical reagents. For chemical modifications: c, control experiment in the absence of chemical reagent; n and d, chemical modifications made under nondenaturing and semi-denaturing conditions, respectively. For DMS, n1 and n2 refer to DMS/RNA ratios of 0.072 μL/μg and 0.144 μL/μg, respectively. In semi-denaturing conditions, the DMS/RNA ratio was of 0.144 μL/μg. Reverse transcription analysis were made with primer 2 (**B**) and primer 3 (**C**). Positions of primers 2 and 3 on the pre-RNA are represented schematically in (**A**). E1 and E2 indicate the position of exon 1 and 2, respectively.

et al., 1992) were subjected in parallel to chemical and enzymatic probing. The results obtained, which are summarized in Figure 1A, confirmed the presence of the 3′-terminal cruciform structure and stem-loop structure 1b in the precursor RNA. Except for an increased intensity of the V1 RNase cleavages in stem-loop 3, the intensities of chemical modifications and enzymatic digestions in the 3′-terminal cruciform structure were very similar for both the mature and precursor RNAs (Fig. 1A). Hence, the secondary structure and the tertiary structure of the 3′ domain were almost identical in the two RNAs. In contrast, the accessibility in stem-loop structure 1b differed at several positions between the precursor and the mature RNA. V1 RNase cleavages were reinforced in the stem and both V1 and S1 cleaved in the terminal loop (Fig. 1A,B). One explanation for the additional V1 cleavages may be that a pseudo-knot structure formed between the 5′-terminal ACUGp sequence of the terminal loop and the CAGUp sequence from position 321 to 324 (Fig. 1A).

A highly folded intron sequence

The enzymatically and chemically modified intron structure was analyzed by reverse transcription with

primers 2 and 3 (Fig. 2) and the results are summarized in Figure 3. Chemical and enzymatic probing experiments clearly demonstrated that the 3′ splice site was located at the 3′ end of a bulged loop in a stem-loop structure designated 1a′. The top part of stem-loop structure 1a′ was identical to that of stem-loop structure 1a in the mature RNA. The branch site sequence (G_{+140}ACUAAC$_{+146}$) was located in a large bulged loop. A long central stem-loop structure was present at the center of the intron from position C_{+31} to G_{+107} (Figs. 2B,C, 3). The base of the stem (segment from position A_{+21} to U_{+25} base paired with the segment from position A_{+109} to U_{+113}) had a lower stability, as reflected by mild chemical modifications in both nondenaturing and semi-denaturing conditions (Fig. 2B). For the 5′-terminal part of the intron, two alternative conformations could fit the experimental results; in the A conformation (Fig. 3A), exon 1 is base paired with the 5′-terminal sequence of the intron, whereas in the B conformation (Fig. 3B), it is base paired with exon 2.

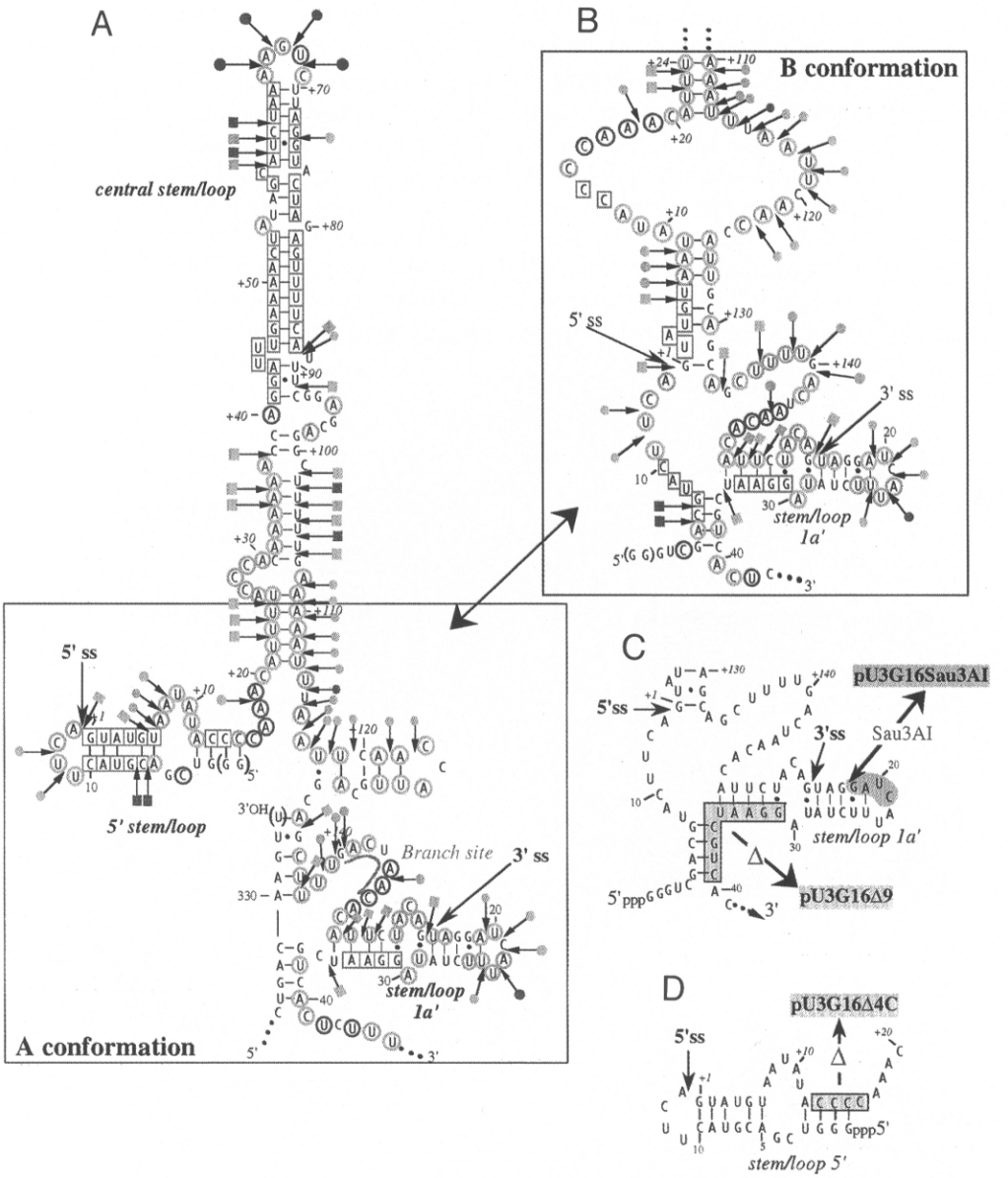

FIGURE 3. Two possible conformations of the intron and exon 1 as deduced from RNA structure-probing experiments. **A:** Structure of the intron and exon 1 in the A conformation. **B:** Differences in the B conformation. Positions of enzymatic cleavages and chemical modifications are indicated with the same nomenclature as in Figure 1A. The 5′ and 3′ splice sites are indicated as 5′ ss and 3′ ss, respectively. **C,D:** Differences between the pU3G16 transcript and the pU3G16Δ9, pU3G16Sau3AI transcripts and the pU3GΔ4C transcript, three variants that were made to distinguish between the two possible conformations.

A base pair interaction between exon 1 and the intron 5′ extremity

Two approaches were used to test whether the V1 RNase cleavages in exon 1 resulted from a base pair interaction with exon 2 or with the intron. In the first approach, a transcript missing the 9-nt sequence of exon 2 that is complementary to exon 1 was produced by site-directed mutagenesis (transcript pU3G16Δ9, Fig. 3C). In the second approach, a transcript missing the exon 2 sequence downstream from position 17 was produced by *Sau*3A I digestion of the DNA template prior to transcription (transcript pU3G16Sau3AI, Fig. 3C). As illustrated in Figure 4A, the patterns of chemical modifications and enzymatic digestions in exon 1 were identical for the transcripts pU3G16, pU3G16Δ9, and pU3G16Sau3AI. Consequently, these three transcripts adopt the A conformation. This suggested that, in the authentic precursor RNA, the 5′-terminal sequence of the intron, which is known to base pair with U1 snRNA in the course of spliceosome assembly (Lerner et al., 1980; Mount et al., 1983; Zhuang & Weiner, 1986), is base paired with exon 1. However, we had to verify that the 5′-terminal structure found in the transcripts was not an artefact due to the presence of the two additional G residues at the 5′ end. Indeed, the resulting run of three G residues at the 5′ end could interact with the run of four C residues between positions C_{+13} and C_{+16} within the intron, and this might favor formation of a 5′ stem-loop structure. Due to the constraints of T7 RNA polymerase, the two additional G residues at the 5′ end of the transcripts could not be omitted. Thus, to check whether the 5′-terminal stem-loop structure was formed in the absence of a base pair interaction between the 5′-terminal G run and the [C_{+13}-C_{+16}] segment, we deleted the C run between positions *+13* and *+16* by site-directed mutagenesis (transcript pU3G16Δ4C, Fig. 3D). The 5′-terminal stem-loop structure in transcript pU3G16Δ4C was still evident in probing experiments (Fig. 4B). Hence, we concluded that this 5′-terminal structure is likely to be present in the authentic pre-U3A snoRNA.

In summary, our probing and site-directed mutagenesis experiments demonstrated the presence of a 5′-terminal stem-loop structure, a central stem-loop structure, and stem-loop structure 1a′ in the pre-U3 snoRNA (Fig. 5). A few additional interactions of low stability were also suggested by the results of the probing experiments (Fig. 5). In particular, a base pair in-

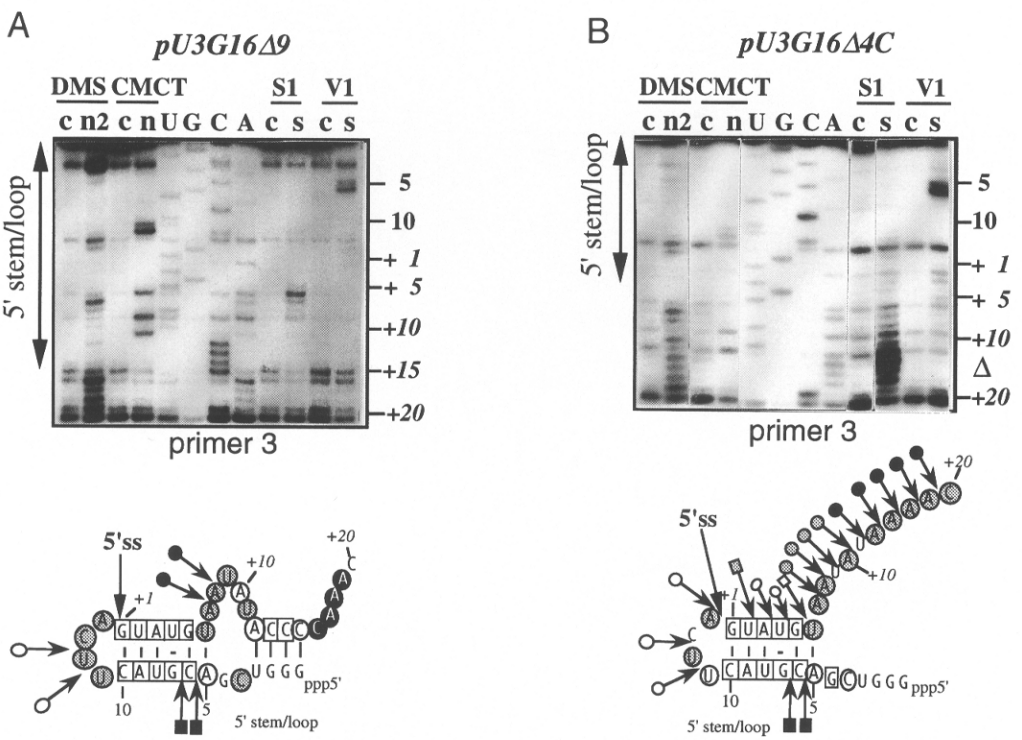

FIGURE 4. Chemical and enzymatic probing of exon 1 structure in the pU3G16Δ9 and pU3G16Δ4C transcripts. Transcripts pU3G16Δ9 (Fig. 3C) and pU3G16Δ4C (Fig. 3D) were subjected to enzymatic digestions and chemical modifications under nondenaturing conditions. **A,B:** Upper: Reverse transcriptase analysis with primer 3 (Fig. 2A). Lower: Results of probing experiments are represented schematically on the proposed structures. Nomenclature is that used in Figure 1A, except that green, orange, and grey are replaced by white, grey, and black, respectively. Boxed nucleotides were shown clearly to be unmodified by chemical reagents. The 5′ splice site is indicated.

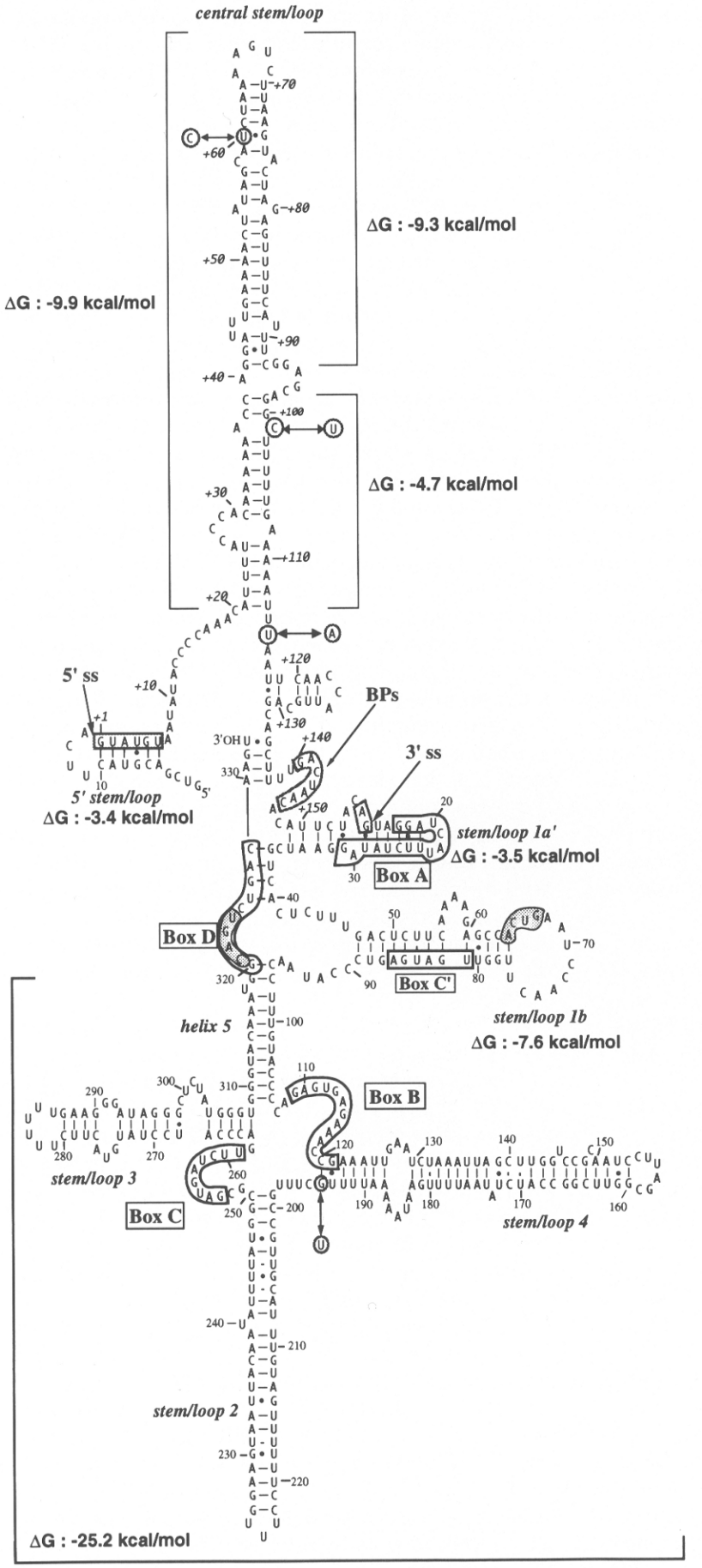

FIGURE 5. Proposed secondary structure model for the pre-U3A snoRNA. The sequence is that of the pre-U3A snoRNA from *S. cerevisiae* FL100 (Myslinski et al., 1990). Differences found in the pre-U3A* snoRNA from *S. cerevisiae* GY5 (Brulé et al., 1995) are indicated by circled nucleotides. Phylogenetically conserved boxes A, B, C, C′, and D, the 5′ and 3′ splice sites, and branch site are boxed. Helix and stem-loop structure numbering is derived from that used in the mature U3A snoRNA. Two nucleotide sequences that may be involved in a pseudoknot structure are shadowed. For the intron central stem-loop structure, the free energies calculated for the entire structure (ΔG on the left), the upper part of the structure, and for the base paired segments at the bottom (ΔGs on the right) are given.

teraction may occur between the GCUUp sequence upstream of the branch site (position G_{+134} to U_{+137}) and the 3′ extremity of exon 2 (Fig. 5). However, due to the presence of an additional U residue at the 3′ end of the transcript, this interaction might be reinforced in the T7 transcript compared to the authentic RNA (Fig. 3A).

In vitro splicing efficiency depends upon the 5′ splice site accessibility and the branch site sequence

Because U3A snoRNA is produced in large amount in yeast, a high efficiency of splicing of the pre-U3A snoRNA is expected in vivo. It was, thus, surprising to find both a noncanonical branch site sequence, GACUAACp (Myslinski et al., 1990), and a base pair interaction between exon 1 and the intron 5′ extremity in the pre-U3A snoRNA. To obtain more information on this observation, in vitro splicing experiments were made with the pU3G16 transcript and a series of variant pU3 transcripts.

Transcript pU3G16 was spliced inefficiently in vitro and this is shown by the very low ratio of mature RNA to precursor RNA (M/P: 0.04) (Fig. 6A). In contrast, a transcript with a 52-nt long extension at the 5′ end of exon 1, which arose from the BS(−) phagemid (transcript pU3G66, Fig. 6A), was spliced very efficiently (M/P: 1.37) (Fig. 6A). The pU3G66 transcript was spliced more efficiently than an actin transcript, which is considered to be one of the more efficiently spliced yeast pre-mRNA in vitro (Lin et al., 1985). This was particularly surprising because of the GACUAACp sequence at the branch site.

Using *S. cerevisiae* thermosensitive mutants with defect in the pre-mRNA splicing machinery (SPJ11.4 and AH rna8; Chang et al., 1988; Jackson et al., 1988), we verified that introns in the pre-U3A snoRNA are spliced by the same machinery as introns in pre-messenger RNAs (not shown).

When the branch site sequence was converted to a canonical one in transcript pU3G16 (transcript designated as pU3U16, Fig. 6A), splicing was increased by a factor of about 15 (Fig. 6A). When the same mutation was performed in transcript pU3G66 (transcript designated as pU3U66), splicing efficiency was only increased by a factor of 1.7 (Fig. 6B). Why was transcript pU3G66 spliced very efficiently with a GACUAACp sequence, whereas transcript pU3G16 needed a UACUAACp branch site sequence for efficient splicing? One possible explanation was the short length of exon 1 in transcript pU3G16, because 16 nt represent the shortest size for a natural yeast exon 1 spliced in a spliceosome (Duchêne et al., 1988). To test for this possibility, a series of chimeric transcripts, with 5′-terminal extensions of different length and sequence, were produced as described in the Materials and methods (Fig. 6A). Transcript pU3G74 has a 60-nt extension, with a sequence different from that of transcript pU3G66. Transcripts pU3G66Δ1 and pU3G66Δ2 differ from transcript pU3G66 by 21- and 29-nt long deletions within the 52-nt extension, respectively. As shown in Figure 6A, no splicing was observed for the pU3G74 transcript and a low level of splicing was obtained for the pU3G66Δ1 and pU3G66Δ2 transcripts (M/P ratios of 0.09 and 0.25, respectively). Hence, splicing efficiency was not correlated to the length of exon 1.

Another possible explanation for the poor splicing efficiency of transcript pU3G16 was the sequestering of the 5′ splice site in the stable stem-loop structure formed at the 5′ end of this transcript. In agreement with this hypothesis, a secondary structure analysis of the pU3G66, pU3G66Δ1, and pU3G66Δ2 transcripts (Fig. 7) showed a reinforced 5′ stem-loop structure in the transcripts that were spliced inefficiently in vitro (pU3G66Δ1 and pU3G66Δ2). In contrast, the 52-nt extension of the efficiently spliced pU3G66 transcript folded on itself independently of the pre-U3A snoRNA sequence (Fig. 7), and this reduced the 5′ stem-loop structure stability. Due to the presence of reverse transcriptase stops in the CCCCp sequence (between positions A_{+12} and A_{+17}) in control experiments, the single-stranded or double-stranded state of this sequence in transcript pU3G66 could not be determined.

Because we showed that, in transcript pU3G16Δ4C, the 5′ stem-loop structure has a lower stability, if the above reasoning was correct, transcript pU3G16Δ4C was expected to be spliced more efficiently than transcript pU3G16. As shown in Figure 6B, this was indeed the case and the splicing efficiency of transcript pU3G16Δ4C is 62% of that measured for transcript pU3G66 (for comparison, the efficiency for pU3U16, in the same experiment, was 42% of that for transcript pU3G66).

Finally, a last confirmation of the strong negative effect of a reinforced 5′ stem-loop structure on pre-U3 snoRNA splicing efficiency was the absence of splicing when the irregular stem of the 5′ stem-loop structure was converted into a perfect 12-bp stem. In this case, splicing was abolished both in the presence of a GACUAACp branch site sequence (transcript pU3G16ds5′) and a canonical branch site sequence (transcript pU3U16ds5′) (Fig. 6B).

As evidenced by a kinetic study of spliceosome assembly with the pU3G66, pU3G16, pU3G16Δ4C, and pU3G16ds5′ transcripts (Fig. 8), an increased sequestration of the 5′ splice site in the 5′ stem-loop structure, in the presence of a noncanonical branch site sequence, affects an early step of spliceosome assembly. After incubation for 10 or 40 min, the rates of B, A1, and A2 complexes formation were reduced strongly for transcript pU3G16, compared to transcripts pU3G66 and pU3G16Δ4C. The A1 and A2 complexes were not even seen in case of transcript pU3G16ds5′.

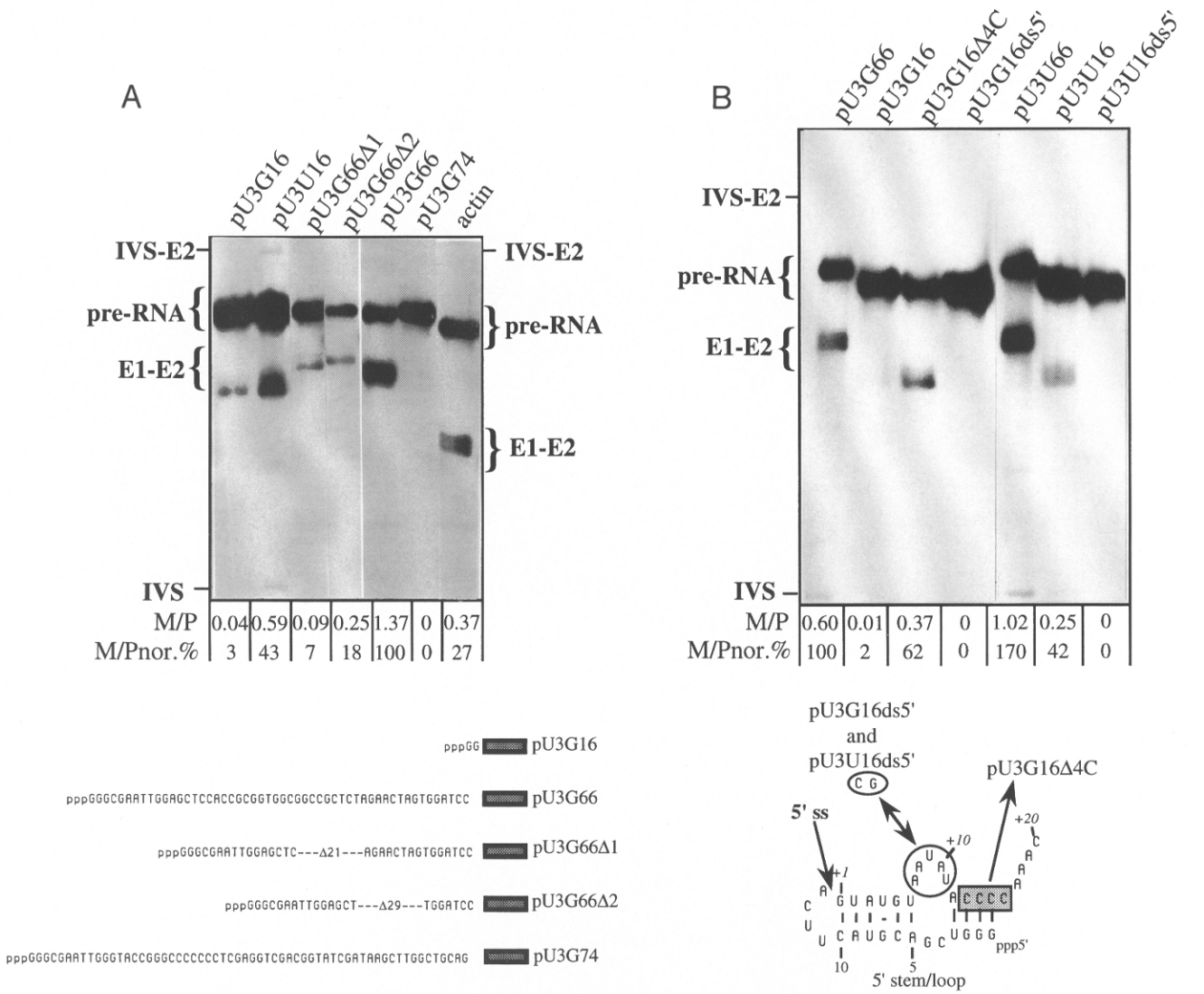

FIGURE 6. Comparative analysis of the in vitro splicing efficiency of the chimeric and variant pre-U3A snoRNA. **A:** Effect of the length and sequence of an extension at the 5′ end of exon 1 is tested. Sequences of the extensions are shown at the bottom and the products of the in vitro splicing reaction are shown above. Products were fractionated by electrophoresis on a 6% polyacrylamide gel under denaturing conditions. An actin transcript was included for comparison. Positions of precursor RNA (pre-RNA), first intermediate (IVS-E2), mature RNA (E1-E2), and intron (IVS) are as indicated. The mature/precursor RNA ratio (M/P) and the values obtained after normalization relative to the M/P ratio of transcript pU3G66 taken as 100% (M/Pnor.%) are given. **B:** Effect of a GACUAACp or UACUAACp branch site sequence in chimeric and variant pre-U3A snoRNA transcripts is tested. The mutation in the pU3G16ds5′ and pU3U16ds5′ transcripts, which convert the irregular stem of the 5′ stem-loop structure into a perfect 12-bp helix, is shown, as well as the four-cytosine deletion in transcript pU3G16Δ4C. Splicing products were analyzed as in A.

DISCUSSION

We established a complete secondary structure model for the pre-U3A snoRNA of *S. cerevisiae*. This is the first complete secondary structure determination of a pre-RNA spliced in a spliceosome. The *S. cerevisiae* pre-U3A snoRNA displays two specific structural features that are not expected for an efficiently spliced transcript: a noncanonical branch site sequence, and a base paired 5′ box. We used site-directed mutagenesis and in vitro splicing experiments to study the influence of these two peculiar features on splicing efficiency. Altogether, the results described in this paper have specific implication for the understanding of U3 snoRNA biogenesis, but also for the understanding of the effect of pre-RNA secondary structure on in vitro splicing efficiency by the yeast splicing machinery.

3′ Domains of the mature and the precursor RNA have similar structures

Most of the secondary structure motifs found in the *S. cerevisiae* U3A snoRNA are found in the precursor RNA. Only the basis of stem-loop structure 1a is not

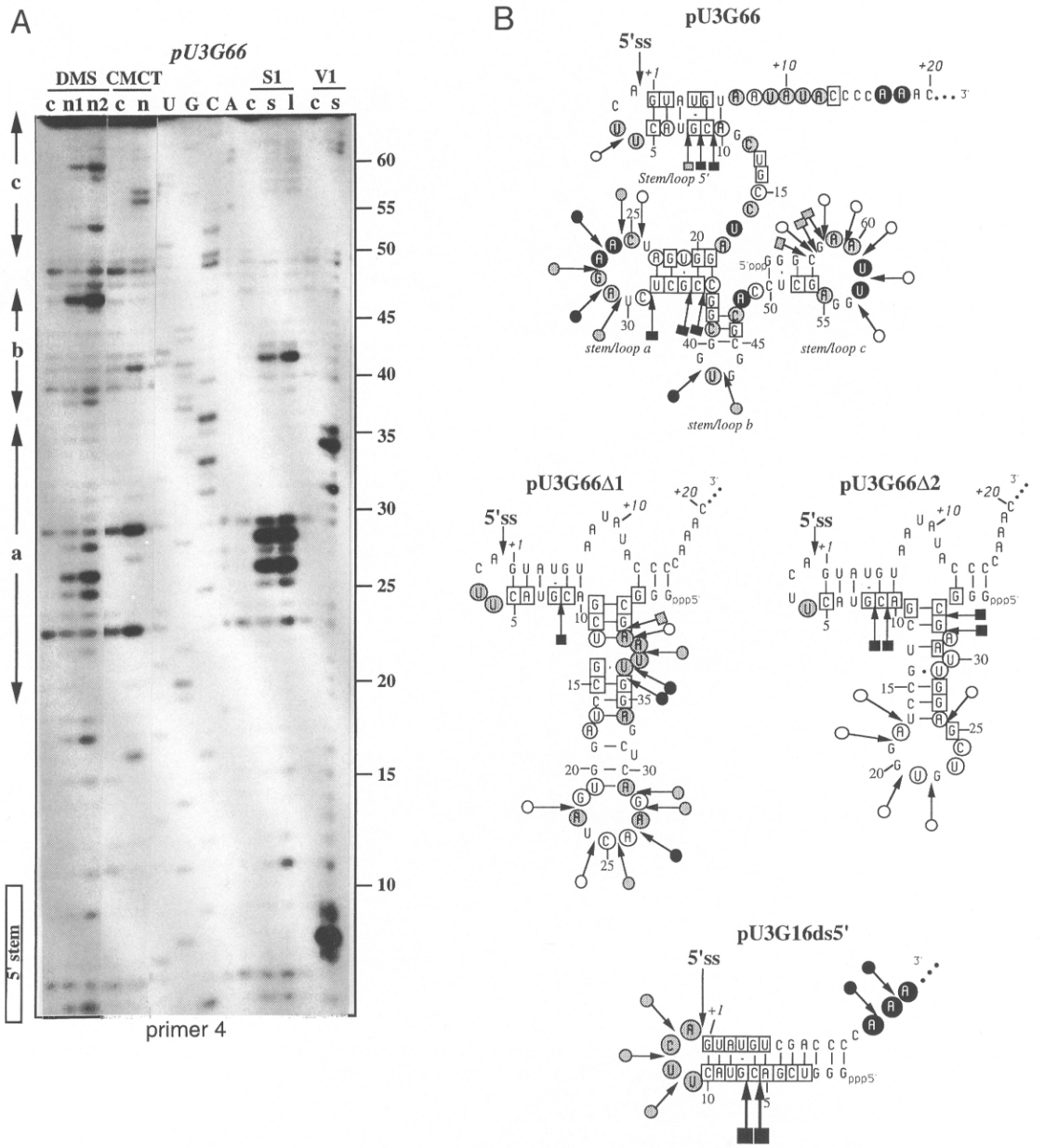

FIGURE 7. Secondary structure analysis of the 5′-terminal extensions. Four transcripts, pU3G66, pU3G66Δ1, pU3G66Δ2, and pU3G16ds5′, were subjected to chemical and enzymatic probing of the RNA structure and the products reverse transcribed. **A:** Primer extension analysis of cleavages and modifications in transcript pU3G66, using primer 4 (same nomenclature as in Figs. 1, 2). **B:** Results obtained for the 5′-terminal region of the four transcripts are represented schematically on the proposed secondary structures. Symbols are as in Figure 4.

formed in the precursor RNA. As a consequence, depending on the relative kinetics of transcription versus spliceosome assembly, splicing of the pre-U3A snoRNA in vivo may take place in the presence of a highly folded exon 2. In addition, because exon 2 contains the sequences expected to bind the U3 snoRNP proteins (Parker & Steitz, 1987; Lübben et al., 1993; Hartshorne & Agabian, 1994; our unpubl. results on the yeast U3 snoRNP), one could not exclude the possibility that splicing of the pre-U3A snoRNA in vivo takes place on a pre-U3A snoRNP complex containing some of the U3A snoRNP proteins.

An intron central stem-loop structure in U3 snoRNA precursors

Several studies have suggested that formation of a base pair interaction between sequences downstream from the 5′ splice site and upstream of the branch site sequence is required for efficient splicing of long introns in *S. cerevisiae* (Pikielny & Rosbash, 1985; Newman, 1987; Parker & Patterson, 1987; Goguel & Rosbash, 1993; Libri et al., 1995). The secondary structure that we have determined for the pre-U3A snoRNA demonstrates that the postulated interaction is formed in this

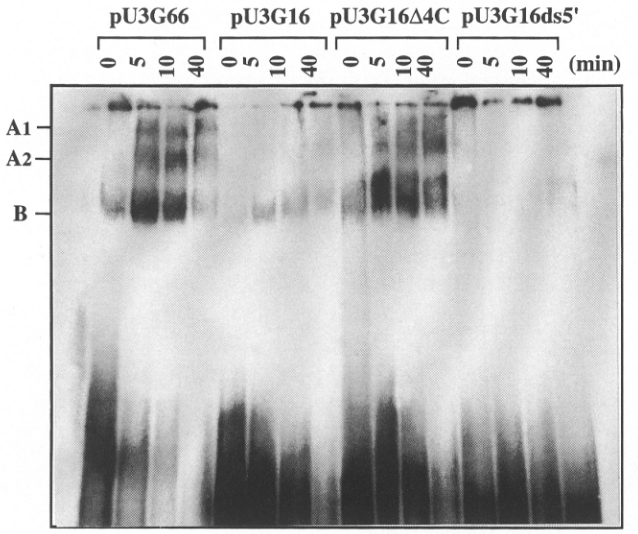

FIGURE 8. Kinetic study of spliceosomal complex assembly on variant and chimeric pre-U3A snoRNAs. Spliceosomal complex assembly was made with nuclear extracts of strain EJ101 under the same conditions as for the splicing assay. Five-microliter aliquots were taken after the indicated times, in minutes of incubation, heparin was added, and the spliceosomal complexes were fractionated on 4% nondenaturing gel. Positions of complexes A_1, A_2, and B (Cheng & Abelson, 1987) are as indicated.

precursor RNA. However, in the pre-U3A snoRNA, this interaction has a low stability as determined by a free energy calculation (Fig. 5) and by the mild accessibility of the base paired segments to chemical reagents, both in nondenaturing and semi-denaturing conditions (Figs. 2, 3). The upper part of the central stem-loop structure of the pre-U3A snoRNA, which is more stable (−9.3 kcal/mol, Fig. 5), is probably required to ensure the proper interactions between the sequences downstream from the 5′ splice site and upstream of the branch site sequence.

An argument in favor of an important biological role of the central stem-loop structure in the pre-U3A snoRNA intron is the possibility to form a similar stem-loop structure with a completely different sequence in the intron of the second U3 snoRNA gene of *S. cerevisiae* (U3B gene) (Brulé et al., 1995). In addition, the *S. cerevisiae* FL100 and *S. cerevisiae* GY5 U3A snoRNA genes differ at three positions in the intron, and two of these mutations reinforce the proposed central stem-loop structure in *S. cerevisiae* GY5 (Brulé et al., 1995; Fig. 5).

Pre-U3A snoRNA is very efficiently spliced despite a noncanonical branch site sequence and a base paired 5′ splice site

Although an artificial 6-bp interaction that involves the 5′ splice site in the RP51A pre-mRNA had a negative effect on in vitro splicing efficiency (Goguel et al., 1993), the pU3G16Δ4C transcript, and particularly the pU3G66 transcript, which bear the naturally occurring 6-bp interaction at the 5′ splice site, were spliced very efficiently in vitro. This is particularly surprising because these two transcripts also have noncanonical branch site sequences.

Interestingly, the 6-bp interaction at the 5′ splice site of the pU3G66 transcript has the same calculated free energy (−3.4 kcal/mol) as the interaction between U1 snRNA and the pre-U3A snoRNA 5′ box. When the stability of the 5′ stem-loop structure was increased by −2.7 kcal/mol, upon formation of three additional G-C base pairs (transcript pU3G16), the in vitro splicing efficiency was reduced by 98% relative to pU3G66. However, converting the branch site into the canonical sequence partially relieved the splicing efficiency to 42% of pU3G66.

Effects of mutations in the branch site sequence on in vitro and in vivo splicing efficiency in yeast were studied previously (Jacquier et al., 1985; Vijayraghavan et al., 1986), but, to our knowledge, the effect of a mutation at the first position was not tested. Our results show that, at least in vitro, the effect of a mutation at this position depends strongly on the pre-RNA conformation.

Based on the unexpectedly high in vitro splicing efficiency of the pU3G66 transcript, the noncanonical branch site sequence and the base paired 5′ box in the pre-U3A snoRNA are probably offset by an optimization of the other structural parameters that influence splicing efficiency, such as the long central stem-loop structure. Interestingly, the branch site sequence is located in a large bulged loop that is closed by a helix of low energy; this helix is probably destabilized easily upon spliceosome assembly. The 3′ splice site is located at the extremity of a bulged loop in the stem-loop structure 1a′. Recent investigations on plants (Liu et al., 1995) and HeLa cells (Smith et al., 1993) showed that sequestrating the 3′ splice site has a milder effect on splicing efficiency than sequestrating the 5′ splice site. This may also be the case for yeast.

The noncanonical branch site and the base paired 5′ splice site in the *S. cerevisiae* pre-U3A snoRNA may provide a control mechanism for U3A snoRNA production at the splicing step. Indeed, our results show that the noncanonical branch site sequence places pre-U3A snoRNA splicing under the dependence of the availability of the 5′ splice site sequence. One may imagine the existence of a negative regulator protein that would bind to the 5′-terminal stem-loop structure and reinforce its stability. As a consequence, splicing efficiency would be reduced strongly. A very similar mechanism explains the retro-control of the *S. cerevisiae* protein RPL 32 at the splicing level (Eng & Warner, 1991; Vilardell & Warner, 1994; Li et al., 1995). An argument in favor of the biological importance of a noncanonical branch site sequence and of the possibility to form a 5′ stem-loop structure in the pre-U3A snoRNA

is the observation of these two features in the pre-U3B snoRNA, in spite of a very high degree of nucleotide sequence divergence of the intron (Brulé et al., 1995).

Altogether, our results reinforced the idea of a strong influence of precursor RNA secondary structure on the efficiency of intron excision by the yeast splicing machinery.

MATERIALS AND METHODS

Strains and growth conditions

E. coli strain TG1 (Gibson, 1984) was used for plasmid DNA preparation and *E. coli* strains HB 2151 and HB 2154 (Carter et al., 1985) for propagation of the M13mp19 bacteriophage. Growth was achieved at 37 °C in Luria Broth Medium with 100 mg/mL of ampicillin added when necessary. For nuclear extract preparation, *S. cerevisiae* strain EJ101 (Lin et al., 1985) and thermosensitive strains SPJ11.4 and AH rna8 (Lustig et al., 1986) were grown according to Lin et al. (1985).

Plasmids and bacteriophages

The pVS1::snR17A plasmid, a pUC18 derivative with an uninterrupted *S. cerevisiae* U3A snoRNA-coding sequence under the control of a T7 promoter (Ségault et al., 1992), was used to produce U3A snoRNA in vitro (U3 transcript). The U3A snoRNA gene (exons 1 and 2, and the intron), which was cloned previously under the control of a T7 promoter in the recombinant bacteriophage M13mp9::T7-snR17A (Ségault et al., 1992), was excised with *Hin*d III nuclease and inserted into plasmid pUC18 that was cleaved with the same enzyme. The resulting plasmid was used to produce pre-U3A snoRNA in vitro (pU3G16 transcripts). The M13mp9::T7-snR17A recombinant phage was also used as a template for site-directed mutagenesis. BS(−) (Short et al., 1988) and SK(+) (Short et al., 1988) plasmids were used for construction of chimeric U3A snoRNA genes. The *Eco*R I–*Sal* I restriction fragment, which contains the *S. cerevisiae* actin intron bordered by portions of exon 1 and exon 2 (Lin et al., 1985), was placed under the control of a T7 promoter by inserting it in the pGEM9Zf(−) plasmid cut with the *Eco*R I and *Sal* I enzymes.

Construction of chimeric U3A snoRNA gene

Chimeric U3A snoRNA genes, with an extended exon 1 (Fig. 6A), were constructed as follows. The 2.2-kb *Sal* I fragment of plasmid pFL1::snR17A (Myslinski et al., 1990) was inserted in the two possible orientations at the *Sal* I restriction site of bacteriophage M13mp9. The two recombinant bacteriophages generated were denoted M13mp9::U3ASalI$^+$ (U3A gene transcription is oriented in the *Hin*d III to *Eco*R I direction as referred to M13mp9 restriction sites) and M13mp9::U3ASalI$^-$ (opposite orientation of the U3A gene). To produce pre-U3A snoRNA with a 60-nt long extension at the 5′ end of exon 1, the 0.81-kb *Hin*d III–*Hpa* I fragment from M13mp9::U3A*Sal* I$^+$, which contained the U3A snoRNA gene, was inserted into plasmid SK(+) cleaved with *Hin*d III and *Sma* I nucleases. The transcript produced from the resulting construct has a 74-nt long exon 1 and was denoted pU3G74. To produce a pre-U3A snoRNA with a 52-nt long 5′-terminal extension of completely different sequence, the 1.05-kb *Bam*H I–*Hin*d III fragment from M13mp9::U3A*Sal* I$^-$ containing the U3A snoRNA gene was inserted into the BS(−) plasmid cleaved with the same enzymes. The transcript produced by the resulting construct had a 66-nt long exon 1 and was denoted pU3G66. Then, truncations were generated within the additional 52-nt segment using a unique *Not* I restriction site, located in the middle of the 52-nt segment, and *Bal* 31 nuclease. Conditions for *Bal* 31 nuclease were as follows: 5 μg of DNA were digested with 0.2 units of *Bal* 31 nuclease, for 1 or 2 min in 10 μL of 0.1 M EDTA, 1 M NaCl, 0.1 M $CaCl_2$, 0.2 M $MgCl_2$, 0.2 M Tris-HCl, pH 8, buffer. After phenol/chloroform extraction and ethanol precipitation, blunt ends were generated with 5 units of the Klenow fragment in 10 μL of 10 mM $MgCl_2$, 50 mM Tris-HCl, pH 7.6, buffer in the presence of 0.05 mM of each dNTP for 30 min at 37 °C. Circularization of the blunt-ended DNA was achieved with T4 DNA ligase under standard conditions (Sambrook et al., 1989). The circularized plasmids were used to transform the *E. coli* TG1 strain. Plasmids were prepared from a series of colonies isolated on LB/ampicillin medium. The extent of deletions was determined by sequence analysis using the dideoxynucleotide method (Sanger et al., 1977). Two plasmids with a 21-nt and 29-nt deletion extension were selected and used to produce chimeric pre-U3A snoRNA; the transcripts produced from these constructs were denoted pU3G66Δ1 and pU3G66Δ2, respectively.

Production of variant U3A snoRNA genes

Site-directed mutageneses were achieved with the method of Kramer et al. (1984), or with the Amersham commercial kit that uses the recombinant phage M13mp9::T7snR17A as a template. Oligonucleotides used in these experiments are listed in Table 1. The variant U3A snoRNA genes were inserted into a pUC18 plasmid after cleavage by *Hin*d III nuclease, as described above for the wild-type gene. Oligonucleotide 5 was used to delete the 9-nt long exon 2 sequence from position 31 to 39, and oligonucleotide 6 to delete the intron sequence from position *+13* to *+16*. Oligonucleotide 3 was used to convert the branch site sequence into a canonical sequence, starting from the pU3G16 or the pU3G66 gene. Finally, oligonucleotide 7 was used to produce a variant pre-U3A snoRNA with a reinforced 5′ stem-loop structure (Fig. 6B); this mutation was made both on the wild-type gene and on the variant gene with a $UACUAAC_p$ sequence at the branch site. The name of the in vitro transcripts produced from these mutated genes are given in Table 1.

In vitro transcription

The *Hpa* I restriction site located at the 3′ end of the U3A coding sequence (Ségault et al., 1992) was used to linearize all DNA templates except the template of transcript pU3G74, which was linearized with the *Bam*H I nuclease. To produce a truncated pU3G16Sau3AI transcript, the *Sau*3A I nuclease was used for template linearization. The pGEM::Actin plasmid was used to produce actin pre-mRNA transcript after linearization with the *Eco*R I nuclease. The digested DNAs were phenol extracted, ethanol precipitated, and dissolved in water.

TABLE 1. Oligonucleotides used for site-directed mutagenesis.[a]

No.	Sequence	Target sequence	Generated mutation	Resulting transcripts
3	5′-ATGTGTTAGTAAAAAGCTGCTG-3′	(+*150*)–(+*129*)	G+*140* → T	pU3U16 and pU3U66
5	5′-GTCAAAGAGTTATAGAAATGAT-3′	(19)–(49)	Δ(G31–C39)	pU3G16Δ9
6	5′-GGGTAAAATGTTTTATATTACATACTG-3′	(13)–(+*29*)	Δ(C+*13*–C+*16*)	pU3G16Δ4C
7	5′-TGTTTGGGGTCGACATACTGAA-3′	(11)–(+*21*)	(A+*7*)–(U+*11*) → CG	pU3G16ds5′ and pU3U16ds5′

[a] Oligonucleotide sequences complementary to the snoRNA gene are underlined and vertical arrows indicate deletions. The exon-targeted sequences are numbered as in the mature U3A snoRNA (Ségault et al., 1992) and nucleotide positions in the intron are numbered by italic numbers from +*1* to +*157*. Nomenclature for transcripts produced from the mutated genes is as follows: pU3 for the pre-U3A snoRNA, G or U for GACUAACp or UACUAACp branch site sequence followed by the size of exon 1 and the identification of the mutation (i.e., Δ4C for deletion of 4 C residues).

Synthesis of cold transcripts for RNA secondary structure-probing experiments was performed in 125 μL of the following buffer: 10 mM NaCl, 10 mM $MgCl_2$, 10 mM DTT, 40 mM Tris-HCl, pH 8, containing 5 μg of linearized plasmid, 62.5 nmol of each ribonucleoside triphosphate, 125 units of RNase Guard™ (Pharmacia), 140 units of T7 RNA polymerase (Amersham). After 2 h of incubation at 37 °C, nucleic acids were phenol extracted and ethanol precipitated. Template DNA was digested with 5 units of RNase-free DNase I (Boehringer) in 250 μL of 5 mM $MgCl_2$, 100 mM sodium acetate, pH 5, buffer for 30 min at 37 °C. After phenol extraction and ethanol precipitation, the RNA (about 10 μg) was dissolved in 120 μL of sterile water; 2 μL of this solution was used for each chemical reaction or enzymatic digestion.

Synthesis of labeled transcripts for in vitro splicing experiments was performed with 0.5 μg of cleaved DNA template in 5 μL of 6 mM $MgCl_2$, 4 mM spermidine, 10 mM DTT, 40 mM Tris-HCl, pH 8, in the presence of 0.5 mM ATP, CTP, and GTP, 0.2 mM UTP, 80 units of T7 RNA polymerase, 10 μCi of [α-^{32}P]UTP (800 Ci/mmol), and 10 units of RNasin. Incubation was at 37 °C for 2 h. Transcription reactions were stopped by adding 5 μL formamide loading buffer. Labeled transcripts were purified by electrophoresis on 6% polyacrylamide gel and were eluted at 4 °C in 0.5 M sodium acetate, 1 mM EDTA, pH 8, in the presence of 2.5% phenol, for 16 h. The RNA from the aqueous phase was ethanol precipitated and dissolved in 50 μL of H_2O for in vitro splicing experiments.

Preparation of splicing extract and in vitro splicing assay

Yeast whole-cell extracts were prepared according to Lin et al. (1985), using either the wild-type strain (EJ101) or the thermosensitive strains (SPJ11.4 and AH rna8). Heat inactivation of the extracts was performed at 30 °C for 30 min, as described previously (Lustig et al., 1986). Splicing assays were conducted in a buffer containing 3 mM $MgCl_2$, 60 mM KPO_4, pH 7, with 1 mM spermidine, 2 mM ATP, 3% PEG, 0.4 nM uncapped transcript, and 40% (v/v) of splicing extract for 1 h at 16 °C, as described previously by Newman et al. (1985). The M/P ratio was evaluated by densitometry of the autoradiogram with the Gel Doc 1,000 UV Fluorescent System (Bio-Rad). Calculations were made with the Bio-Rad software, taking into account the lengths of the mature and precursor RNAs.

Nondenaturing gel electrophoresis of splicing complexes

Complex assembly analysis was performed as described previously by Cheng and Abelson (1987). RNA transcripts were incubated under the splicing conditions described above. Five-microliter aliquots were recovered after 0, 5, 10, and 40 min of incubation. Heparin, at a concentration of 2 μg/μL of whole cell extract, was added to these aliquots as described by Cheng and Abelson (1987), and the material was fractionated on a 4% nondenaturing polyacrylamide gel (acrylamide/bisacrylamide, 80:1) made in 1 mM EDTA, 20 mM Tris-HCl, pH 8, buffer. Gels were run at 25 V/cm for 5 h at 4 °C, and were dried prior to autoradiography.

Chemical modifications

Chemical modifications were performed either under nondenaturing conditions or under semi-denaturing conditions (Ehresmann et al., 1987; Ségault et al., 1992). Each modification was performed on about 200 ng of in vitro synthesized RNA in the presence of 5 μg of a commercial yeast tRNA mixture (Boehringer). Prior to the chemical reaction, the RNA was dissolved in 100 μL of the appropriate buffer and preincubated 10 min at 20 °C (temperature used for the modification reactions). DMS modifications under nondenaturing conditions were made in 50 mM KCl, 10 mM $MgCl_2$, 100 mM sodium cacodylate, pH 7.5, buffer and under semi-denaturing conditions in 2 mM EDTA, 100 mM sodium cacodylate, pH 7.5, buffer, with either 0.75 μL of pure DMS or 0.75 μL of a DMS solution (1:1, v/v; DMS/EtOH) per assay. The incubation was for 15 min, and the reaction was stopped by ethanol precipitation. The RNA was washed with 70% ethanol and dissolved in 14 μL of H_2O. Seven microliters of this solution were used for a reverse transcriptase elongation assay. CMCT modifications under nondenaturing conditions were made in 50 mM KCl, 10 mM $MgCl_2$, 100 mM sodium borate, pH 8, buffer, and under semi-denaturing conditions,

in the same buffer except that 2 mM EDTA were used instead of 10 mM $MgCl_2$ and 50 mM KCl, with 1.05 or 2.1 mg of CMCT per 100-μL assay. Incubation was for 30 min. At the end of the reaction, the same procedure was used as for DMS modification.

Enzymatic cleavages

As for chemical modifications, the enzymatic digestions were performed on T7 RNA transcripts mixed with 5 μg of commercial tRNA. V1 RNase was prepared from *Naja oxiana* venom (Vassilenko & Babkina, 1965). RNA was pre-incubated 10 min at 0 °C in 10 μL of reaction buffer (350 mM KCl, 10 mM $MgCl_2$, 10 mM Tris-HCl, pH 7.5). Incubation was for 2, 7, or 10 min with an enzyme/RNA ratio of 1.2 unit/μg. The reaction was stopped by adding 5 μL of 100 mM EDTA, followed by phenol extraction. RNAs digested for 2 and 7 min were mixed. After ethanol precipitation, RNA was washed with 70% ethanol, and subjected to primer extension analysis. S1 nuclease was from Pharmacia. RNA was pre-incubated 10 min at 20 °C in 10 μL of reaction buffer (50 mM KCl, 10 mM $MgCl_2$, 1 mM $ZnCl_2$, 25 mM Na acetate, pH 4.5). Incubation was for 12 or 25 min at 20 °C with 2 units of enzyme. The reaction was stopped by adding 2 μL of 100 mM EDTA, extracted with phenol, and the RNA was prepared for primer extension analysis as above.

Primer extension analysis

Chemical modifications and enzymatic cleavages in the pre-U3A snoRNA transcripts were analyzed with reverse transcriptase. The oligonucleotide primers used were complementary to the pre-U3A snRNA sequences from position 319 to 333 (primer 1), 92 to 106 (primer 2), *+129* to *+150* (primer 3), and *+1* to *+19* (primer 4). Primer oligonucleotides were 5′ end-labeled with [γ-^{32}P] ATP (Amersham), 3,000 mCi/mmol. They were annealed to 7-μL aliquots of the RNA samples described above for 10 min at 65 °C in 40 mM KCl, 6 mM $MgCl_2$, 50 mM Tris-HCl, pH 8.3, buffer, and the solution was cooled to room temperature. Reverse transcription was performed with 1 unit of Rous sarcoma virus 2 reverse transcriptase (Amersham) or 1 unit of Avian myeloblastosis virus reverse transcriptase (Life Science), for 30 min at 45 °C, in the presence of 125 μM of each dNTP. To prepare sequencing ladders of unmodified RNA, dideoxynucleotide:deoxynucleotide mixtures (in a 1:2 ratio) were used. Reverse transcripts were fractionated by electrophoresis on a 7% polyacrylamide sequencing gel (Sambrook et al., 1989).

Estimation of RNA secondary structure stability

Estimation of stem-loop structure stability was made with the Mfold program of the GCG software, version 8.1 Unix (1995), which is based on the thermodynamic values proposed by Jeager et al. (1989) for an RNA in solution in 1 M NaCl buffer at 37 °C.

ACKNOWLEDGMENTS

J. Bayeul is thanked for her excellent technical assistance and Kyle Tanner for reading the manuscript. A. Grégoire, V. Ségault, R. Fournier, and F. Brulé were fellows of the French Ministère de la Recherche et de l'Enseignement Supérieur. This work was supported by the Centre National de la Recherche Scientifique and the French Ministère de la Recherche et de l'Enseignement Supérieur.

Received March 22, 1996; returned for May 3, 1996; revised manuscript received August 15, 1996

REFERENCES

Beltrame M, Tollervey D. 1992. Identification and functional analysis of two U3 binding sites on yeast pre-ribosomal RNA. *EMBO J 11*:1531–1542.

Beltrame M, Tollervey D. 1995. Base pairing between U3 and the pre-ribosomal RNA is required for 18S rRNA synthesis. *EMBO J 14*: 4350–4356.

Brulé F, Grégoire A, Ségault V, Mougin A, Branlant C. 1995. Secondary structure conservation of the U3 small nucleolar RNA introns in *Saccharomyces*. *C R Acad Sci Paris, Life Sciences 318*:1197–1206.

Carter P, Bedouelle H, Winter G. 1985. Improved oligonucleotide site-directed mutagenesis using M13 vectors. *Nucleic Acids Res 13*: 4431–4443.

Chang TH, Clark MW, Lustig AJ, Cusick ME, Abelson J. 1988. RNA11 protein is associated with the yeast spliceosome and is localized in the periphery of the cell nucleus. *Mol Cell Biol 8*:2379–2393.

Cheng SC, Abelson J. 1987. Spliceosome assembly in yeast. *Genes & Dev 1*:1014–1027.

Clouet d'Orval B, d'Aubenton Carafa Y, Sirand-Pugnet P, Gallego M, Brody E, Marie J. 1991. RNA secondary structure repression of a muscle-specific exon in HeLa cell nuclear extracts. *Science 252*:1823–1828.

Craig N, Kass S, Sollner-Webb B. 1987. Nucleotide sequence determining the first cleavage site in the processing of mouse precursor rRNA. *Proc Natl Acad Sci USA 84*:629–633.

Deshler JO, Rossi JJ. 1991. Unexpected point mutations activate cryptic 3′ splice sites by perturbing a natural secondary structure within a yeast intron. *Genes & Dev 5*:1252–1263.

Duchêne M, Low A, Schweizer A, Domdey H. 1988. Molecular consequences of truncations of the first exon for in vitro splicing of yeast actin pre-mRNA. *Nucleic Acids Res 16*:7233–7239.

Ehresmann C, Baudin F, Mougel M, Romby P, Ebel JP, Ehresmann B. 1987. Probing the structure of RNAs in solution. *Nucleic Acids Res 15*:9109–9128.

Eichler DC, Craig N. 1994. Processing of eukaryotic ribosomal RNA. *Prog Nucleic Acid Res Mol Biol 49*:197–239.

Eng FJ, Warner JR. 1991. Structural basis for the regulation of splicing of a yeast messenger RNA. *Cell 65*:797–804.

Gibson TJ. 1984. Studies on the Epstein Barr virus genome [thesis]. Cambridge, UK: Cambridge University.

Goguel V, Rosbash M. 1993. Splice site choice and splicing efficiency are positively influenced by pre-mRNA intramolecular base pairing in yeast. *Cell 72*:893–901.

Goguel V, Wang Y, Rosbash M. 1993. Short artificial hairpins sequester splicing signals and inhibit yeast pre-mRNA splicing. *Mol Cell Biol 13*:6841–6848.

Hartshorne T, Agabian N. 1994. A common core structure for U3 small nucleolar RNAs. *Nucleic Acids Res 22*:3354–3364.

Hawkins JD. 1988. A survey on intron and exon lengths. *Nucleic Acids Res 16*:9893–9908.

Hughes JM, Ares M. 1991. Depletion of U3 small nucleolar RNA inhibits cleavage in the 5′ external transcribed spacer of yeast pre-ribosomal RNA and impairs formation of 18S ribosomal RNA. *EMBO J 10*:4231–4239.

Jackson SP, Lossky M, Beggs JD. 1988. Cloning of the RNA8 gene of *Saccharomyces cerevisiae*, detection of the RNA8 protein, and demonstration that it is essential for nuclear pre-mRNA splicing. *Mol Cell Biol 8*:1067–1075.

Jacquier A, Rodriguez JR, Rosbash M. 1985. A quantitative analysis of the effects of 5′ junction and TACTAAC box mutants and mutant combinations on yeast mRNA splicing. *Cell 43*:423–430.

Jeager JA, Turner DH, Zucker M. 1989. Improved predictions of secondary structures for RNA. *Proc Natl Acad Sci USA 86*:7706–7710.
Kalogeropoulos A. 1995. Automatic intron detection in nuclear DNA sequences of *Saccharomyces cerevisiae*. *Yeast 11*:555–565.
Kass S, Craig N, Sollner-Webb B. 1987. Primary processing of mammalian rRNA involves two adjacent cleavages and is not species specific. *Mol Cell Biol 7*:2891–2898.
Kass S, Tyc K, Steitz JA, Sollner-Webb B. 1990. The U3 small nucleolar ribonucleoprotein functions in the first step of preribosomal RNA processing. *Cell 60*:897–908.
Kramer B, Kramer W, Fritz HJ. 1984. Different base/base mismatches are corrected with different efficiencies by the methyl-directed DNA mismatch-repair system of *E. coli*. *Cell 38*:879–887.
Lerner MR, Boyle JA, Mount SM, Wolin SL, Steitz JA. 1980. Are snRNP involved in splicing? *Nature 283*:220–224.
Li H, Dalal S, Kohler J, Vilardell J, White SA. 1995. Characterization of the pre-mRNA binding site for yeast ribosomal protein L32: The importance of a purine-rich internal loop. *J Mol Biol 250*:447–459.
Libri D, Stutz F, McCarthy T, Rosbash M. 1995. RNA structural patterns and splicing: Molecular basis for an RNA-based enhancer. *RNA 1*:425–436.
Lin RJ, Newman AJ, Cheng SC, Abelson J. 1985. Yeast mRNA splicing in vitro. *J Biol Chem 260*:14780–14792.
Liu HX, Goodall GJ, Kole R, Filipowicz W. 1995. Effects of secondary structure on pre-mRNA splicing: Hairpins sequestering the 5′ but not the 3′ splice site inhibit intron processing in *Nicotiana plumbaginifolia*. *EMBO J 14*:377–388.
Lübben B, Marshallsay C, Rottmann N, Lührmann R. 1993. Isolation of U3 snoRNP from CHO cells: A novel 55 kDa protein binds to the central part of U3 snoRNA. *Nucleic Acids Res 21*:5377–5385.
Lustig AJ, Lin RJ, Abelson J. 1986. The yeast RNA gene products are essential for mRNA splicing in vitro. *Cell 47*:953–963.
Maxwell ES, Fournier MJ. 1995. The small nucleolar RNA. *Annu Rev Biochem 67*:6523–6527.
Miller AM. 1984. The yeast MATa1 gene contains two introns. *EMBO J 3*:1061–1065.
Mizuta K, Hashimoto T, Otaka E. 1992. Yeast ribosomal proteins: XIII. *Saccharomyces cerevisiae* YL8A gene, interrupted with two introns, encodes a homologue of mammalian L7. *Nucleic Acids Res 20*: 1011–1016.
Mougey EB, Pape LK, Sollner-Webb B. 1993. A U3 small nuclear ribonucleoprotein-requiring processing event in the 5′ external transcribed spacer of *Xenopus* precursor rRNA. *Mol Cell Biol 13*: 5990–5998.
Mount SM, Petterson I, Hinterberger M, Karmas A, Steitz JA. 1983. The U1 small nuclear RNA protein complex selectively binds a 5′ splice site in vitro. *Cell 33*:509–518.
Myslinski E, Ségault V, Branlant C. 1990. An intron in the genes for U3 small nucleolar RNAs of the yeast *Saccharomyces cerevisiae*. *Science 247*:1213–1216.
Newman A. 1987. Specific accessory sequences in *Saccharomyces cerevisiae* introns control assembly of pre-mRNAs into spliceosomes. *EMBO J 6*:3833–3839.
Newman AJ, Lin RJ, Cheng SC, Abelson J. 1985. Molecular consequences of specific intron mutations on yeast mRNA splicing in vivo and in vitro. *Cell 42*:335–344.
Parker KA, Steitz JA. 1987. Structural analysis of the human U3 ribonucleoprotein particle reveal a conserved sequence available for base pairing with pre-rRNA. *Mol Cell Biol 7*:2899–2913.
Parker R, Patterson B. 1987. Architecture of fungal introns: Implications for spliceosome assembly. In: Inouye M, Dubock B, eds. *Molecular biology of RNA, new perspectives*. New York: Academic Press. pp 133–148.
Pikielny CW, Rosbash M. 1985. mRNA splicing efficiency in yeast and the contribution of nonconserved sequences. *Cell 41*:119–126.
Raué HA, Planta RJ. 1995. The pathway to maturity: Processing of ribosomal RNA in *Saccharomyces cerevisiae*. *Gene Expression*. Forthcoming.
Sambrook J, Fritsch EF, Maniatis T. 1989. *Molecular cloning. A laboratory manual*. Cold Spring Harbor, New York: Cold Spring Harbor Laboratory Press.
Sanger F, Nicklen S, Coulson AR. 1977. DNA sequencing with chain-terminating inhibitors. *Proc Natl Acad Sci USA 74*:5463–5467.
Ségault V, Mougin A, Grégoire A, Banroques J, Branlant C. 1992. An experimental study of *Saccharomyces cerevisiae* U3 snRNA conformation in solution. *Nucleic Acids Res 20*:3443–3451.
Short JM, Fernandez JA, Sorge JA, Huse WD. 1988. Lambda ZAP: A bacteriophage Lambda expression vector with in vivo excision properties. *Nucleic Acids Res 16*:7583–7600.
Smith CW, Chu TT, Nadal-Guinard B. 1993. Scanning and competition between AGs are involved in 3′ splice site selection in mammalian introns. *Mol Cell Biol 13*:4939–4952.
Takahashi Y, Urushiyama S, Tani T, Ohshima Y. 1993. An mRNA-type intron is present in the *Rhodotorula hasegawae* U2 small nuclear RNA gene. *Mol Cell Biol 13*:5613–5619.
Tani T, Ohshima Y. 1989. The gene for the U6 small nuclear RNA in fission yeast has an intron. *Nature 337*:87–90.
Tani T, Ohshima Y. 1991. mRNA-type introns in U6 small nuclear RNA genes: Implications for the catalysis in pre-mRNA splicing. *Genes & Dev 5*:1022–1031.
Teare J, Wollenzien P. 1989. Structures of human and rabbit β-globin precursor messenger RNAs in solution. *Biochemistry 28*:6208–6219.
Teare J, Wollenzien P. 1990. The structure of a pre-mRNA molecule in solution determined with a site directed cross-linking reagent. *Nucleic Acids Res 18*:855–864.
Vassilenko SK, Babkina GT. 1965. *Biokymiya 30*:705–716.
Vijayraghavan U, Parker R, Tamm J, Iimura Y, Rossi J, Abelson J, Guthrie C. 1986. Mutations in conserved intron sequences affect multiple steps in the yeast splicing pathway, particularly assembly of the spliceosome. *EMBO J 5*:1683–1695.
Vilardell J, Warner JR. 1994. Regulation of splicing at an intermediate step in the formation of the spliceosome. *Genes & Dev 8*: 211–220.
Zhuang Y, Weiner AM. 1986. A compensatory base change in U1 snRNA suppresses a 5′ splice site mutation. *Cell 46*:827–835.